Electronic Supplementary Material (ESI) for Chemical Communications.

A Supramolecular Helicate with Two Independent Fe(II) Switchable Centres and a $[Fe(anilate)_3]^{3-}$ Guest

Leoní A. Barrios,*[a,b] Simon. J. Teat,[c] Olivier Roubeau*[d,e] and Guillem Aromí*[a,b]

SUPPORTING INFORMATION

Synthesis

Ligand L2 (3,3'-bis(3-(pyridin-2-yl)-1H-pyrazol-5-yl)-1,1'-biphenyl) as previously reported by us,[1] while $[(Ph)_4P]_3[Fe(H_2An)_3]$ was prepared according to a published procedure.[2]

$[Fe(anilate)_3]@[Fe_2(L2)_3](BF_4)$ (1)

Inside a glovebox, a suspension of ligand L2 (25 mg, 3 mmol) in dry methanol (10 mL) was added dropwise under stirring to a solution of $Fe(BF_4)_2{\cdot}6H_2O$ (12.8 mg, 2 mmol) in dry methanol (5 mL). The resulting orange slightly cloudy solution was then stirred for 30 minutes. A dark red solution of $[(Ph)_4P]_3[Fe(anilate)_3]$ (15.6 mg, 1mmol) in dry methanol (5 mL) was slowly mixed with the previous slurry during a 10 min. period, producing the precipitation of a greenish solid that was separated by filtration using a glass syringe provided with a filter (0.2 μm pore size). The dark orange filtrate obtained was poured in glass tubes for slow evaporation in air, yielding red orange crystals in form of blocks after 15 days. The yield was 24% (9mg). Elemental analysis calcd. for $C_{102}H_{66}BF_4Fe_3N_{18}O_{12}{\cdot}11H_2O$; MW=2188 (found): C= 55.99 (55.42); H= 4.05 (3.34); N= 11.52 (11.67).

Physical characterization

Magnetic measurements were performed with a commercial magnetometer equipped with a SQUID sensor hosted by the Physical Measurements Unit of the Servicio General de Apoyo a la Investigación-SAI, Universidad de Zaragoza. Dry polycrystalline solid was measured in a gelatin capsule, while fresh crystals were measured within little mother solution sealed in polypropylene bags. Corrections for the sample holder and solution were applied, as determined empirically. The diamagnetic contributions to the compound susceptibility were corrected using Pascal's constant tables.

Differential Scanning Calorimetry (DSC) experiments were done with a Q1000 calorimeter from TA Instruments equipped with the LNCS accessory. Calibration of the temperature and enthalpy scales was achieved with a standard sample of In, using its melting transition (156.6 °C, 3296 $Jmol^{-1}$). Mechanically crimped Al pans with an empty pan as a reference were used. Data were obtained at a scanning rate of 10 $Kmin^{-1}$.

---

[1] M. Darawsheh, L. A. Barrios, O. Roubeau, S. J. Teat, G. Aromí, *Angew. Chem., Int. Ed.* **2018**, *57*, 13509-13513

[2] M. Atzori, L. Marchio, R. Clérac, A. Serpe, P. Deplano, N. Avarvari, M. L. Mercuri, *Cryst. Growth Des.* **2014**, 14, 5938−5948

Single-crystal X-ray diffraction (SCXRD)

Data for desolvated **1** [Fe(anilate)$_3$]@[Fe$_2$(L2)$_3$](BF$_4$) were collected at variable temperatures at Beamline 12.2.1 of the Advanced Light Source (Berkeley, USA), on a Bruker D8 diffractometer equipped with a PHOTON II detector and using silicon (111) monochromated synchrotron radiation (λ = 0.7288 Å). Crystals were left at room temperature in paratone N grease, resulting in desolvation. Data reduction and absorption corrections for this set of data were performed with respectively SAINT and SADABS.[3] Data for fresh solvated crystals of **1** [Fe(anilate)$_3$]@[Fe$_2$(L2)$_3$](BF$_4$)·3MeOH were acquired at variable temperatures on the BL13-XALOC beamline[4] of the ALBA synchrotron (λ = 0.72932 Å). Data reduction and absorption corrections were done with autoproc package,[5] XDS,[6] XIA2[7] and AIMLESS.[8] All structures were solved by intrinsic phasing with SHELXT[9] and refined by full-matrix least-squares on F^2 with SHELXL.[10]

All details can be found in CCDC 2260940-2260952 (fresh solvated **1**, crystal 1), CCDC 2261719-2261733 (fresh solvated **1**, crystal 2) and CCDC 2261757-2261767 (desolvated **1**) which contain the supplementary crystallographic data for this paper. These data can be obtained free of charge from The Cambridge Crystallographic Data Center via https://summary.ccdc.cam.ac.uk/structure-summary-form. Crystallographic and refinement parameters are summarized in Tables S1-S3.

[3] a) G. M. Sheldrick, *SAINT and SADABS*, 2012, Bruker AXS Inc., Madison, Wisconsin, USA; b) L. Krause, R. Herbst-Irmer, G. M. Sheldrick, D. Stalke, *J. Appl. Cryst.*, 2015, **48**, 3-10.
[4] J. Juanhuix, F. Gil-Ortiz, G. Cuní, C. Colldelram, J. Nicolás, J. Lidón, E. Boter, C. Ruget, S. Ferrer and J. Benach, *J. Synchrotron Radiat.*, 2014, **21** , 679-689.
[5] C. Vonrhein, C. Flensburg, P. Keller, A. Sharff, O. Smart, W. Paciorek, T. Womack, and G. Bricogne, *Acta Cryst. D,* 2011, **67**, 293-302.
[6] W. Kabsch, *Acta Cryst. D* 2010, **66**, 125-132.
[7] a) G. Winter, J. Appl. Cryst., 2010, 43, 186-190; b) G. Winter, D. G. Waterman, J. M. Parkhurst, A. S. Brewster, R. J. Gildea, M. Gerstel, L. Fuentes-Montero, M. Vollmar, T. Michels-Clark, I. D Young, N. K Sauter, G. Evans, *Acta Cryst. D*, 2018, **74**, 85-97.
[8] P. R. Evans, G. N. Murshudov, *Acta Cryst. D*, 2013, **69**, 1204-1214.
[9] G. M. Sheldrick, *Acta Cryst. A* 2015, **71**, 3-8.
[10] G. M. Sheldrick, *Acta Cryst. C* 2015, **71**, 3-8.

Table S1. Crystallographic and refinement parameters for the structures of fresh solvated **1** [Fe(anilate)$_3$]@[Fe$_2$(L2)$_3$](BF$_4$)·3MeOH at variable temperatures, crystal 1. The average Fe-N bond lengths for the two Fe(II) sites and the N···O separations for the pyrazole-anilate hydrogen bonds are also given. The data is presented in the same order as the thermal history, from left to right, starting at 100 K. All details can be found in CCDC 2260940-2260952.

Formula	$C_{84}H_{60}Fe_2N_{18}$, $C_{18}H_6FeO_{12}$, BF_4, x(CH_4O)												
T (K)	100(2)	200(2)	300(2)	320(2)	330(2)	340(2)	350(2)	360(2)	380(2)	350(2)	320(2)	300(2)	200(2)
x	3	3	3	2.7	2.593	2.286	1.885	1.386	0	0	0	0	0
FW (g mol^{-1})	2086.21	2086.21	2086.21	2076.62	2073.17	2063.34	2050.48	2034.50	1990.08	1990.08	1990.08	1990.08	1990.08
λ (Å)	0.72932												
Crystal system	cubic												
Space group	$P2_13$												
Z	4												
a (Å)	21.727(3)	21.827(3)	21.855(3)	21.611(3)	21.579(3)	21.599(3)	21.625(3)	21.692(3)	21.785(3)	21.769(3)	21.743(3)	21.719(3)	21.626(3)
V (Å^3)	10257(4)	10399(4)	10439(4)	10093(4)	10048(3)	10076(3)	10113(4)	10207(4)	10339(4)	10316(4)	10279(4)	10245(4)	10114(4)
ρ_{calcd} (g/cm^3)	1.351	1.333	1.327	1.367	1.370	1.359	1.347	1.324	1.279	1.281	1.286	1.290	1.307
μ (mm^{-1})	0.531	0.523	0.521	0.521	0.541	0.539	0.536	0.530	0.521	0.522	0.524	0.525	0.532
Reflections	7555	8996	9009	8704	8674	8696	8713	8828	8920	8877	8851	8844	8753
R_{int}	0.0233	0.0242	0.0260	0.0225	0.0270	0.0236	0.0240	0.0240	0.0235	0.0213	0.0196	0.0192	0.0220
Restraints	245	242	89	91	83	83	91	84	76	76	76	76	84
Parameters	530	530	476	476	477	479	477	477	446	458	458	458	458
Flack x	0.0080(5)	0.073(4)	0.081(4)	0.078(3)	0.059(3)	0.068(3)	0.075(3)	0.094(4)	0.081(4)	0.075(3)	0.079(3)	0.076(3)	0.066(3)
S	1.039	1.076	1.040	1.058	1.052	1.084	1.054	1.048	1.054	1.053	1.052	1.036	1.063
R_1 [I>2σ(I)]	0.0837	0.0554	0.0487	0.0402	0.0319	0.0323	0.0345	0.0455	0.0416	0.0353	0.0315	0.0329	0.0310
wR_2 [I>2σ(I)]	0.2413	0.1647	0.1382	0.1134	0.0926	0.0959	0.1074	0.1342	0.1322	0.1108	0.0977	0.0986	0.0895
R_1 [all data]	0.0855	0.0559	0.0492	0.0408	0.0321	0.0327	0.0353	0.0472	0.0436	0.0365	0.0323	0.0335	0.0312
wR_2 [all data]	0.2480	0.1660	0.1397	0.1143	0.0930	0.0965	0.1086	0.1373	0.1359	0.1128	0.0988	0.0994	0.0897
Largest peak / hole (e Å^3)	0.951 / –0.465	0.934 / –0.265	0.587 / –0.278	0.346 / –0.260	0.208 / –0.218	0.182 / –0.194	0.217 / –0.169	0.314 / –0.305	0.229 / –0.415	0.202 / –0.350	0.168 / –0.388	0.235 / –0.307	0.262 / –0.323
<Fe1-N> (Å)	1.97(1)	1.974(6)	1.985(4)	1.993(4)	1.995(3)	2.000(4)	2.006(4)	2.019(4)	2.036(5)	2.008(4)	1.993(4)	1.988(4)	1.983(3)
<Fe2-N> (Å)	1.96(2)	1.981(7)	2.002(6)	2.071(4)	2.090(4)	2.094(4)	2.099(5)	2.091(6)	2.096(6)	2.067(4)	2.034(4)	2.020(4)	1.985(4)
N3···O1 (Å)	2.926(7)	2.930(3)	2.932(3)	2.940(2)	2.943(2)	2.943(2)	2.942(2)	2.929(3)	2.922(3)	2.906(3)	2.898(2)	2.893(2)	2.888(2)
N4···O2 (Å)	2.918(7)	2.929(3)	2.957(3)	2.995(3)	3.002(2)	3.002(2)	2.994(3)	2.982(3)	2.986(3)	2.973(3)	2.967(2)	2.960(2)	2.943(2)

Table S2. Crystallographic and refinement parameters for the structures of fresh solvated **1** [Fe(anilate)$_3$]@[Fe$_2$(L2)$_3$](BF$_4$)·3MeOH at variable temperatures, crystal 2. The average Fe-N bond lengths for the two Fe(II) sites and the N···O separations for the pyrazole-anilate hydrogen bonds are also given. The data is presented in the same order as the thermal history, from left to right, starting at 250 K. All details can be found in CCDC 2261719-2261733.

Formula	$C_{84}H_{60}Fe_2N_{18}$, $C_{18}H_6FeO_{12}$, BF_4, x(CH_4O)														
T (K)	250(2)	280(2)	300(2)	310(2)	320(2)	325(2)	330(2)	340(2)	350(2)	360(2)	370(2)	380(2)	400(2)	350(2)	300(2)
x	3	3	3	3	3	2.445	2.407	2.272	1.872	1.550	0	0	0	0	0
FW (g/mol)	2086.21	2086.21	2086.21	2086.21	2086.21	2068.42	2067.41	2062.89	2050.06	2039.78	1990.08	1990.08	1990.08	1990.08	1990.08
λ (Å)	0.72932														
Crystal system	cubic														
Space group	$P2_13$														
Z	4														
a (Å)	22.009(3)	21.957(3)	21.828(3)	21.634(3)	21.578(3)	21.573(3)	21.579(3)	21.604(3)	21.631(3)	21.662(3)	21.731(3)	21.768(3)	21.809(3)	21.772(3)	21.725(3)
V (Å^3)	10661(4)	10586(4)	10400(4)	10125(4)	10047(3)	10040(3)	10048(3)	10083(4)	10121(4)	10165(4)	10262(4)	10315(4)	10373(4)	10320(4)	10254(4)
ρ_{calcd} (g/cm^3)	1.300	1.309	1.332	1.369	1.379	1.368	1.366	1.358	1.345	1.333	1.288	1.282	1.274	1.281	1.289
μ (mm^{-1})	0.511	0.514	0.523	0.538	0.542	0.541	0.540	0.538	0.536	0.533	0.525	0.522	0.519	0.522	0.525
Reflections	9197	9109	8999	8759	8663	8650	8677	8710	8764	8767	8482	8533	8252	8870	8837
R_{int}	0.0328	0.0257	0.0264	0.0262	0.0186	0.0236	0.0251	0.0374	0.0314	0.0330	0.0263	0.0261	0.0206	0.0191	0.0194
Restraints	88	85	103	85	92	92	84	84	92	84	484	84	76	76	76
Parameters	476	466	476	466	478	479	479	479	479	477	458	458	459	458	459
Flack x	0.054(3)	0.076(4)	0.092(4)	0.113(4)	0.083(3)	0.064(3)	0.066(3)	0.049(4)	0.063(4)	0.074(4)	0.090(4)	0.071(4)	0.079(3)	0.077(3)	0.081(3)
S	1.100	1.070	1.045	1.049	1.057	1.065	1.074	1.072	1.067	1.027	1.056	1.046	1.042	1.048	1.025
R_1 [I>2σ(I)]	0.0510	0.0498	0.0503	0.0671	0.0356	0.0329	0.0341	0.0378	0.0400	0.0439	0.0506	0.0444	0.0413	0.0362	0.0340
wR_2 [I>2σ(I)]	0.1445	0.1428	0.1412	0.1767	0.1016	0.0930	0.0947	0.1068	0.1131	0.1242	0.1442	0.1323	0.1333	0.1133	0.1035
R_1 [all data]	0.0511	0.0500	0.0508	0.0688	0.0361	0.0332	0.0344	0.0384	0.0410	0.0455	0.0525	0.0468	0.0432	0.0373	0.0346
wR_2 [all data]	0.1447	0.1435	0.1425	0.1803	0.1024	0.0934	0.0951	0.1076	0.1143	0.1266	0.1477	0.1362	0.1376	0.1153	0.1044
Largest peak / hole (e Å^3)	0.780 / –0.410	0.668 / –0.313	0.644 / –0.293	0.646 / –0.673	0.272 / –0.277	0.243 / –0.217	0.264 / –0.254	0.230 / –0.271	0.325 / –0.297	0.264 / –0.302	0.354 / –0.258	0.393 / –0.316	0.254 / –0.363	0.302 / –0.329	0.283 / –0.373
<Fe1-N> (Å)	1.973(4)	1.980(4)	1.990(4)	1.985(6)	1.992(4)	1.994(3)	1.996(3)	2.003(4)	2.006(4)	2.015(4)	2.027(6)	2.034(5)	2.045(6)	2.008(4)	1.988(4)
<Fe2-N> (Å)	1.972(6)	1.982(6)	2.008(6)	2.045(8)	2.077(4)	2.085(4)	2.090(4)	2.096(4)	2.100(4)	2.100(6)	2.100(6)	2.104(6)	2.115(6)	2.063(4)	2.018(4)
N3···O1 (Å)	2.951(3)	2.944(2)	2.932(3)	2.934(3)	2.942(2)	2.944(2)	2.942(2)	2.945(2)	2.947(2)	2.936(3)	2.932(3)	2.931(3)	2.925(3)	2.907(3)	2.891(2)
N4···O2 (Å)	2.920(3)	2.935(3)	2.960(3)	2.993(4)	2.995(2)	3.002(2)	3.002(2)	3.003(3)	2.996(3)	2.990(3)	2.976(4)	2.980(3)	2.975(3)	2.971(3)	2.961(2)

Table S3. Crystallographic and refinement parameters for the structures of desolvated **1** [Fe(anilate)$_3$]@[Fe$_2$(L2)$_3$](BF$_4$) at variable temperatures. The average Fe-N bond lengths for the two Fe(II) sites and the N···O separations for the pyrazole-anilate hydrogen bonds are also given. The data is presented in the same order as the thermal history, from left to right, starting at 300 K. All details can be found in CCDC 2261757-2261767.

Formula	$C_{84}H_{60}Fe_2N_{18}$, $C_{18}H_6FeO_{12}$, BF_4										
FW (g mol^{-1})	1990.08										
λ (Å)	0.72932										
Crystal system	cubic										
Space group	$P2_13$										
Z	4										
T (K)	300(2)	370(2)	400(2)	390(2)	325(2)	290(2)	270(2)	250(2)	190(2)	150(2)	110(2)
a (Å)	21.6924(5)	21.7604(5)	21.7661(4)	21.7575(3)	21.7017(3)	21.6790(3)	21.6594(3)	21.6411(3)	21.5786(3)	21.5393(4)	21.4991(4)
V (Å^3)	10207.6(7)	10303.9(7)	10312.0(6)	10299.8(4)	10220.7(4)	10188.7(4)	10161.1(4)	10135.3(4)	10047.8(4)	9993.0(6)	9937.1(6)
ρ_{calcd} (g/cm^3)	1.295	1.283	1.282	1.283	1.293	1.297	1.301	1.304	1.316	1.323	1.330
μ (mm^{-1})	0.526	0.521	0.521	0.522	0.526	0.527	0.529	0.530	0.535	0.538	0.541
Reflections	7528	5490	5322	5285	6254	6488	6479	7482	8353	7381	8615
R_{int}	0.0271	0.0188	0.0238	0.0213	0.0205	0.0222	0.0223	0.0220	0.0230	0.0188	0.0193
Restraints	51	60	61	61	60	51	60	60	60	60	60
Parameters	457	457	457	457	457	457	457	457	445	457	457
Flack x	0.023(3)	0.017(3)	0.022(3)	0.025(3)	0.016(3)	0.021(3)	0.021(3)	0.025(3)	0.023(2)	0.024(2)	0.0271(18)
S	1.075	1.057	1.055	1.045	1.049	1.037	1.040	1.036	1.040	1.074	1.054
R_1 [$I>2\sigma(I)$]	0.0353	0.0290	0.0314	0.0294	0.0292	0.0299	0.0298	0.0315	0.0333	0.0316	0.0316
wR_2 [$I>2\sigma(I)$]	0.0912	0.0839	0.0901	0.0831	0.0823	0.0825	0.0822	0.0918	0.0946	0.0891	0.0910
R_1 [all data]	0.0372	0.0309	0.0337	0.0311	0.0314	0.0318	0.0313	0.0329	0.0351	0.0321	0.0322
wR_2 [all data]	0.0928	0.0856	0.0920	0.0846	0.0839	0.0841	0.0834	0.0931	0.0963	0.0896	0.0914
Largest peak / hole (e Å^3)	0.472 / –0.260	0.206 / –0.295	0.204 / –0.300	0.202 / –0.219	0.283 / –0.235	0.349 / –0.192	0.284 / –0.242	0.363 / –0.281	0.404 / –0.317	0.413 / –0.397	0.502 / –0.367
<Fe1-N> (Å)	1.984(4)	2.023(6)	2.048(6)	2.041(6)	1.990(4)	1.982(4)	1.981(4)	1.979(4)	1.980(4)	1.978(4)	1.976(4)
<Fe2-N> (Å)	2.013(4)	2.087(6)	2.108(6)	2.101(6)	2.035(6)	2.005(4)	1.993(4)	1.987(4)	1.980(4)	1.979(4)	1.978(4)
N3···O1 (Å)	2.885(3)	2.906(3)	2.920(4)	2.917(3)	2.888(3)	2.884(3)	2.880(3)	2.877(3)	2.880(3)	2.882(3)	2.884(2)
N4···O2 (Å)	2.955(3)	2.973(3)	2.976(4)	2.972(3)	2.960(3)	2.950(3)	2.945(3)	2.940(3)	2.933(3)	2.928(3)	2.923(2)

Table S4. Fe-O and O-C Bond distances (Å) describing the $[Fe(anilate)_3]^{3-}$ guest in the structures of solvated **1** $[Fe(anilate)_3]@[Fe_2(L2)_3](BF_4)\cdot 3MeOH$ at 100 K and desolvated **1** $[Fe(anilate)_3]@[Fe_2(L2)_3](BF_4)$ at 110 K, compared with those of the same species in the starting salt $[(Ph)_4P]_3[Fe(anilate)_3]$.[2]

	$[Fe(anilate)_3]@[Fe_2(L2)_3](BF_4)\cdot 3MeOH$	$[Fe(anilate)_3]@[Fe_2(L2)_3](BF_4)$	$[(Ph)_4P]_3[Fe(anilate)_3]$[a]
Fe3–O1	2.012(4)	1.9995(16)	2.010
Fe3–O2	1.996(4)	1.9879(16)	1.995
O1–C29	1.300(7)	1.310(3)	1.294
O2–C30	1.296(8)	1.309(3)	1.295
O3–C33	1.237(18)	1.223(3)	1.236
O4–C34	1.231(19)	1.219(3)	1.229

[a] Average values for the three inequivalent anilate ions

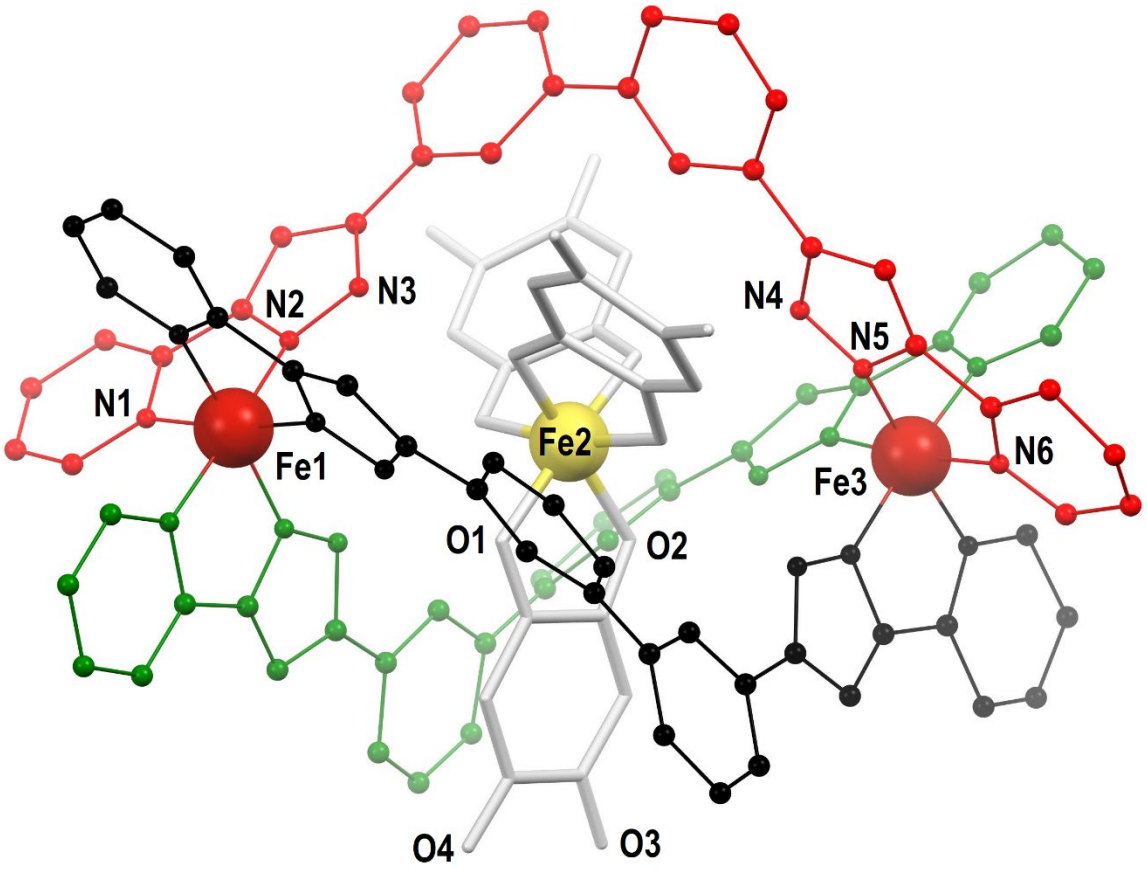

Figure S1. Representation of the supramolecular assembly $([Fe(anilate)_3]@[Fe_2(L2)_3])^+$ of **1**·3MeOH. Only independent heteroatoms labelled. Each L2 ligand is in a different color (red, black and green). The central $[Fe(anilate)_3]^{3-}$ moiety is in capped sticks style. H atoms are not shown.

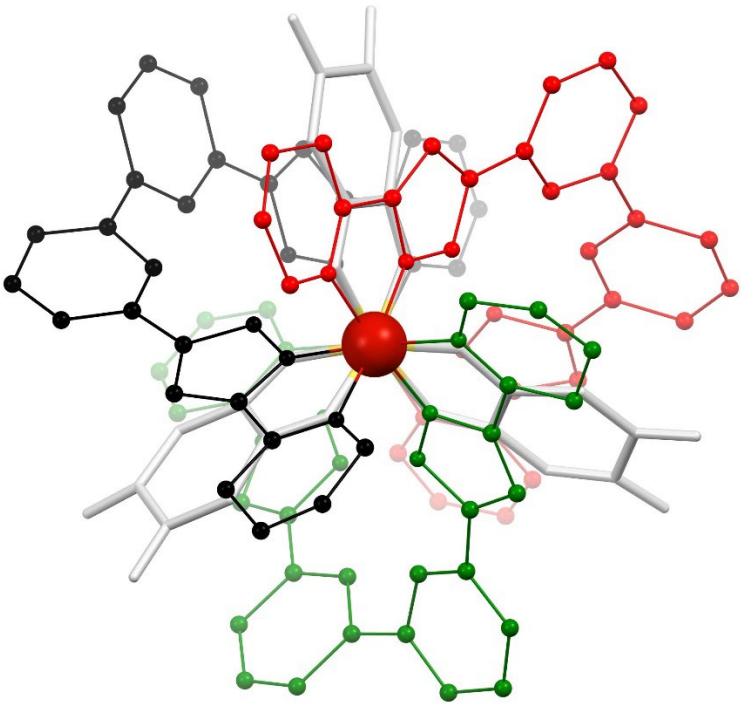

Figure S2. Representation of the supramolecular assembly $([Fe(anilate)_3]@[Fe_2(L2)_3])^+$ of **1**·3MeOH, approximately down the molecular axis. Same colouring scheme as in Fig. S1. H atoms are not shown.

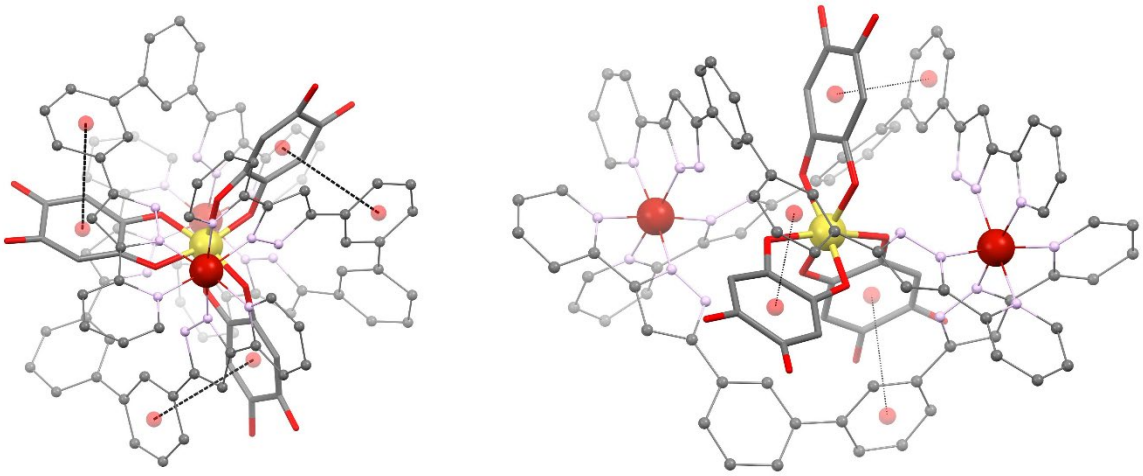

Figure S3. Same views of the supramolecular assembly $([Fe(anilate)_3]@[Fe_2(L2)_3])^+$ of **1**·3MeOH as in Figs S1 and S2, highlighting the π···π interactions involving the anilate rings of the guest and one of the phenyl rings of ligands L2.

Behaviour of fresh crystals of 1 (with three lattice MeOH molecules)

SCXRD measurements at variable temperatures were also performed on crystals of **1** not exposed to air. This was done by recovering crystals within their mother solution with the oil drop method using paraton N grease and mounting them rapidly within the cryostream at 100 K. Two sets of measurements were done on two different crystals and showed good reproducibility (Figs S4 and S5, Tables S1 and S2).

Upon warming (Fig. S4), a sharp increase of the Fe2-N bond distances is observed above 300 K, concomitant with a decrease of the cubic cell parameter *a*. In the same temperature range, the unique crystallographic lattice MeOH molecule becomes more diffuse (300 K), and then, it is not present anymore (above 360 K). The occupation of this lattice methanol was therefore refined in this range of temperature, and indeed it decreases in agreement with a progressive loss of lattice solvent (see Table S1 and S2). A small decrease of the Fe2-N bond distances is then observed above *ca.* 350 K, corresponding with the full loss of lattice MeOH, and then coinciding with the temperature dependence observed for desolvated **1**. Interestingly, the N4···O2 separation describing the pyrazole-anilate hydrogen bond on the Fe2 side of the helicate host exhibits very similar temperature dependence as that of the Fe2-N bond, while the N3···O1 separation describing the pyrazole-anilate hydrogen bond on the Fe1 side remains largely unaffected.

Upon cooling the temperature dependences of the Fe-N bond distances, hydrogen bonds N···O separations and cell parameter are the same as those observed for a crystal exposed to desolvation *before* measurements (Fig. S5).

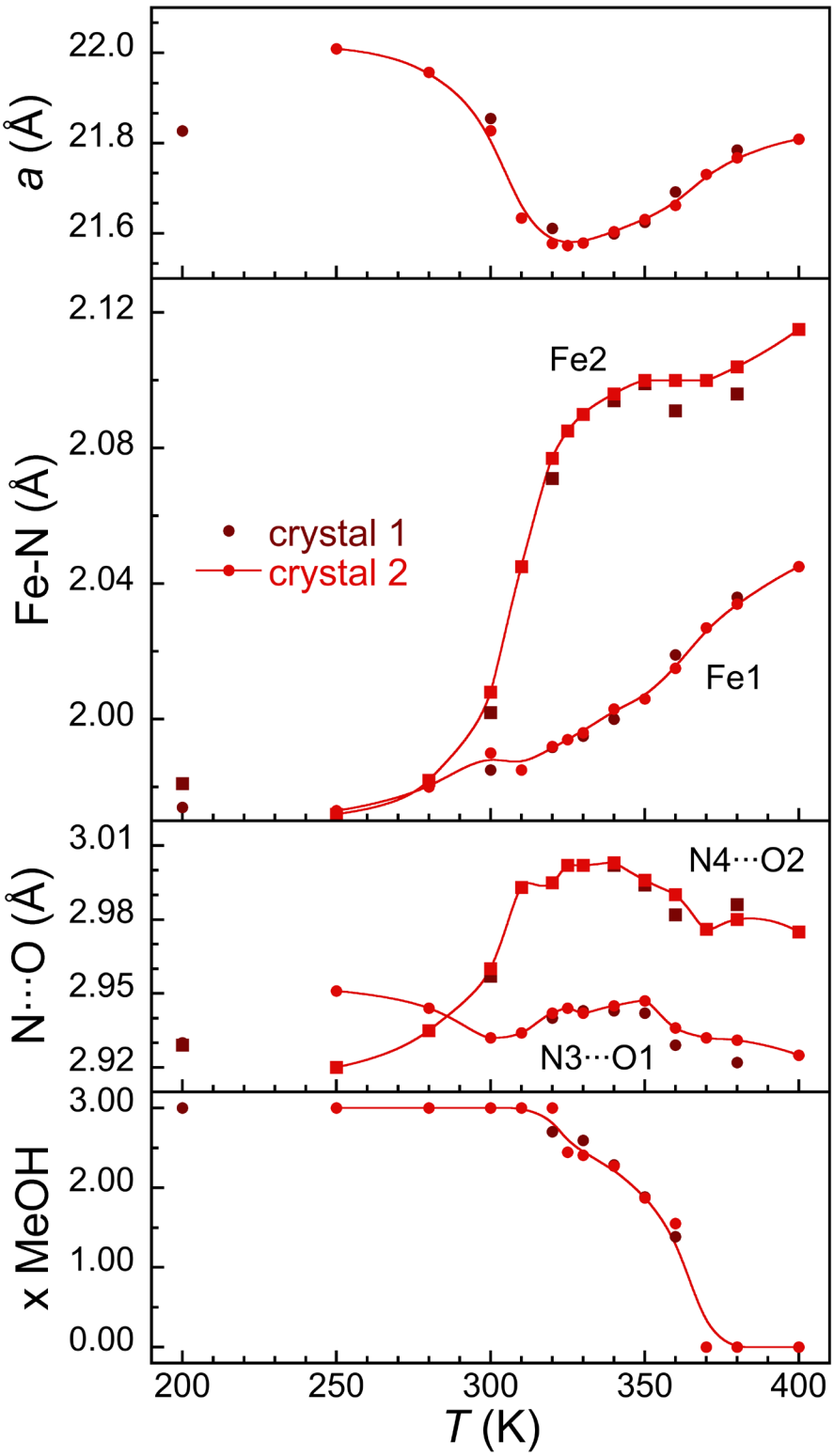

Figure S4. Temperature dependence upon warming of the cell parameter *a*, average Fe-N bond lengths for the two Fe(II) sites, N···O separations for the pyrazole-anilate hydrogen bonds and lattice methanol content for two crystals of fresh solvated **1** $[Fe(anilate)_3]@[Fe_2(L2)_3](BF_4)\cdot 3MeOH$. Lines are a guide to the eye based on crystal 2 data.

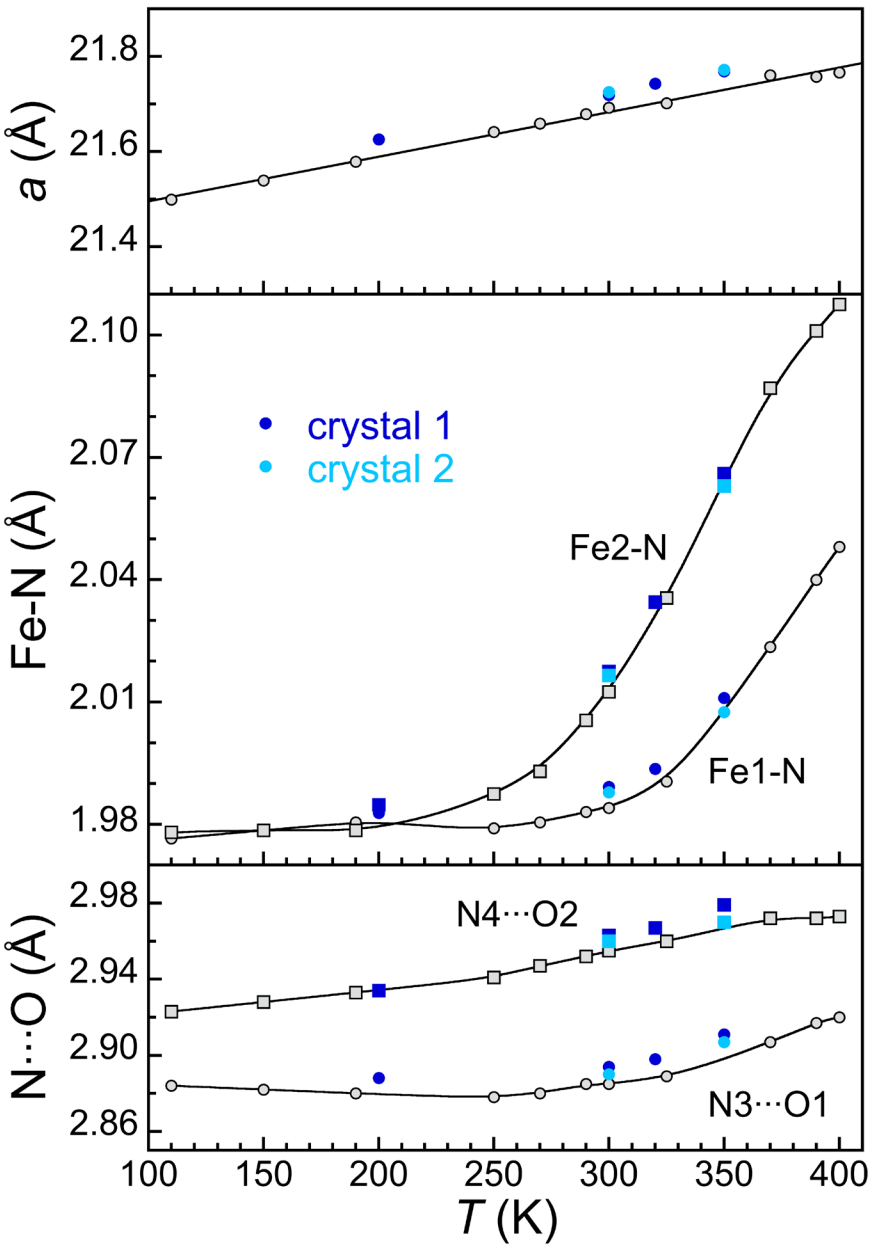

Figure S5. Temperature dependence upon cooling of the cell parameter *a*, average Fe-N bond lengths for the two Fe(II) sites and N···O separations for the pyrazole-anilate hydrogen bonds for two crystals of fresh solvated **1** $[Fe(anilate)_3]@[Fe_2(L2)_3](BF_4)\cdot 3MeOH$, after warming to 380 (crystal 1) and 400 K (crystal 2). For comparison, the temperature dependence of the same parameters for a crystal of desolvated **1** $[Fe(anilate)_3]@[Fe_2(L2)_3](BF_4)$ are shown as grey symbols. Lines are a linear fit in the case of the cell parameter *a*, and otherwise only a guide to the eye.

These structural observations are paralleled by magnetic measurements of crystals in contact with their MeOH mother solution within sealed polypropylene bags. This is because the seal does not withstand temperatures close to the boiling point of MeOH, resulting in removal of the little amount of solution and the crystals eventually loosing their lattice MeOH (the magnetometer sample chamber is filled with He gas at sub-atmospheric pressure), at similar temperatures as the single crystals protected with paraton N grease.

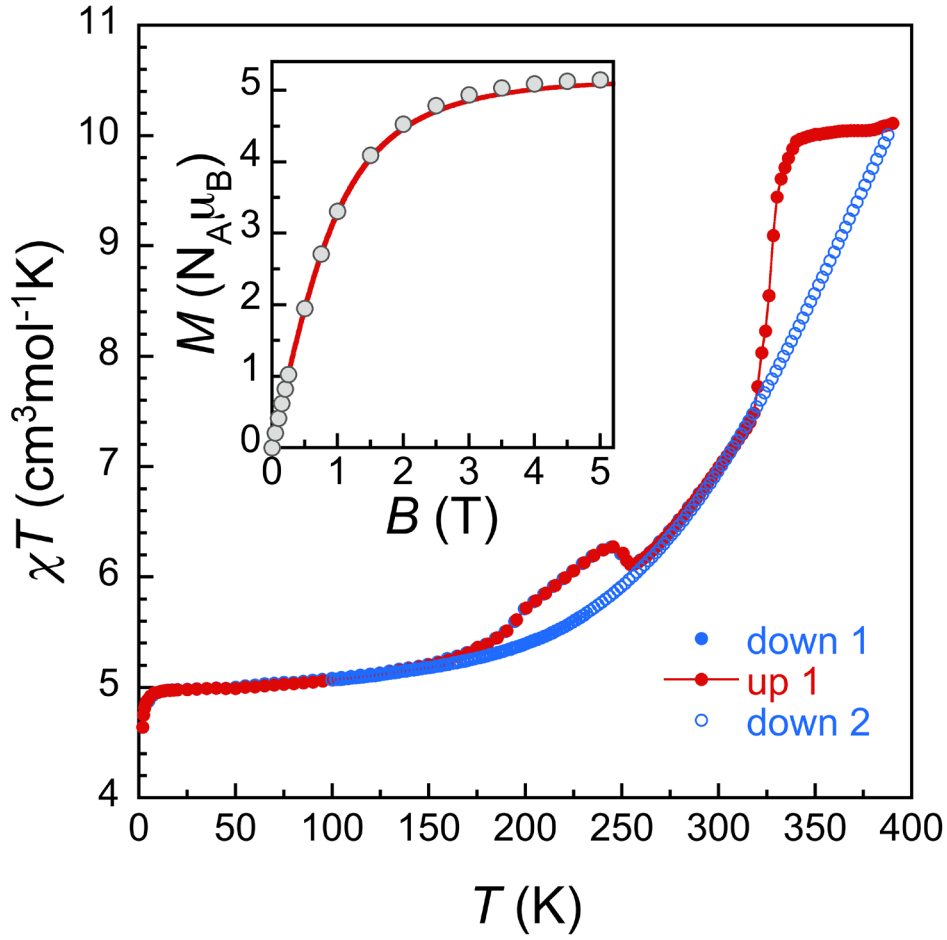

Figure S6. Temperature dependence of χT (χ is the molar magnetic susceptibility) over a cooling-warming-cooling temperature scan starting at 300 K for fresh solvated crystals of **1** [Fe(anilate)$_3$]@[Fe$_2$(L2)$_3$](BF$_4$)·3MeOH initially sealed within a polypropylene bag with a small amount of their mother MeOH solution. During the warming scan, the seal broke resulting in evaporation of the small amount of solvent and desolvation of crystals. Inset: magnetization *vs.* field data obtained at 5 K, before the warming scan. The red line is the Brillouin function for S = 5/2 and g = 2.06 at this temperature.

The first cooling-warming cycle below 300 K shows a gradual thermal spin-crossover (SCO) but still very partial at 300 K, as depicted through the thermal dependence of the product χT (Fig. S6, χ is the molar magnetic susceptibility). This behavior and the low temperature plateau at *ca.* 5.03 cm^{3}mol^{-1}K are in good agreement with the data obtained on desolvated crystals. The isothermal magnetization data at 2 K (inset in Fig. S6) agrees well with the Brillouin function of S = 5/2 and g = 2.06. The broad hump observed in the range 175-260 K is

likely solely due to the presence of the solution MeOH (MeOH melting occurs at 191 K) and its effect on the signal of paramagnetic crystals in it.

Upon heating above 300 K, a sharp jump occurs that can reasonably be ascribed to the loss of lattice solvent and its effect on the spin-crossover of the Fe(II) ions, likely mostly on the Fe2 site. Further cooling shows again a gradual SCO, which is then reproducible, and remains incomplete at 400 K. The absence of a hump in the 175-260 K range confirms the loss of MeOH solution.

Eventually, differential scanning calorimetry measurements were performed on fresh crystals of solvated **1** [Fe(anilate)$_3$]@[Fe$_2$(L2)$_3$](BF$_4$)·3MeOH that support the structural and magnetic observations (Fig. S7).

Crystals were taken out of the mother MeOH solution, placed in an Al pan, which was crimped once the solvent had evaporated and mass was stable. The crimped Al pan was immediately placed in the DSC oven at 25ºC, and measurements were started right away. The Al pan crimp being non-hermetic and the DSC oven being under a flow of N2, crystals of **1** are then likely subject to loss of their lattice MeOH.

Indeed, the first warming scan shows a very broad and energetic anomaly starting just above 300 K, which can reasonably be ascribed to vaporization of remaining traces of solvent and loss and vaporization of lattice MeOH of the crystals of **1**. Further cooling-warming scans are virtually feature-less, except for a possible very broad and weak anomaly in the range 300-430 K that could correspond to the SCO process of the desolvated crystals of **1** [Fe(anilate)$_3$]@[Fe$_2$(L2)$_3$](BF$_4$).

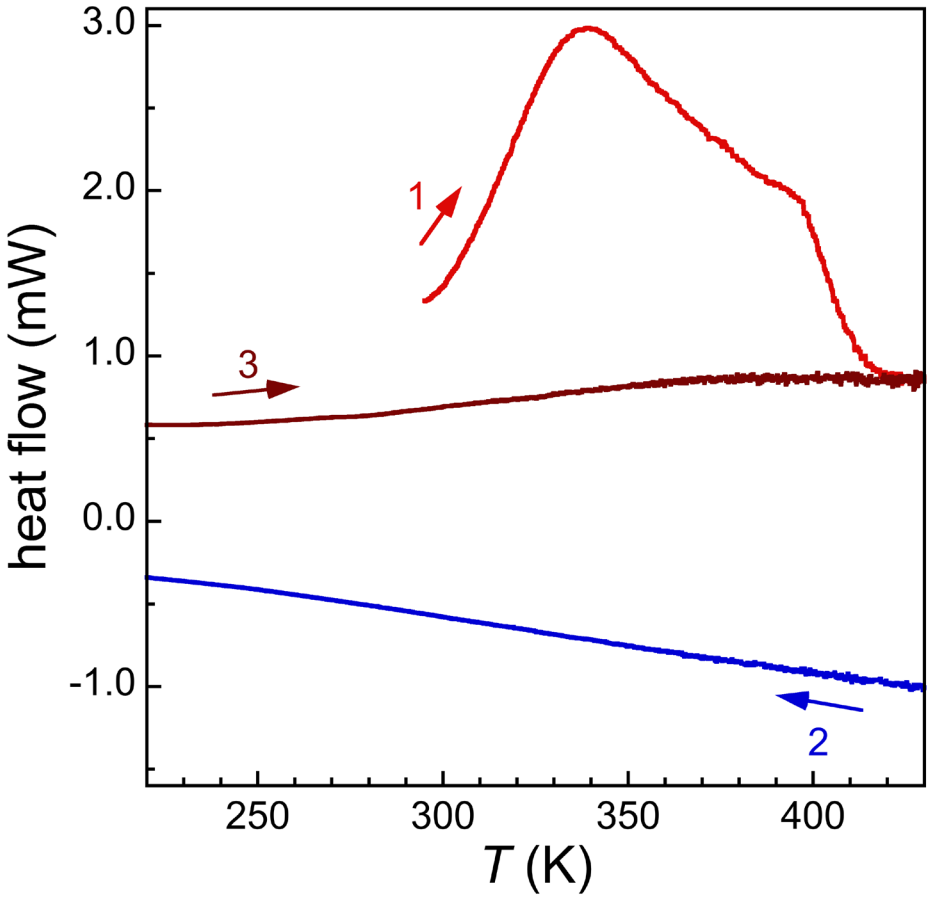

Figure S7. DSC traces over a cooling-warming-cooling temperature scan starting at 293 K for fresh solvated crystals of **1** [Fe(anilate)$_3$]@[Fe$_2$(L2)$_3$](BF$_4$)·3MeOH crimped within an Al pan.

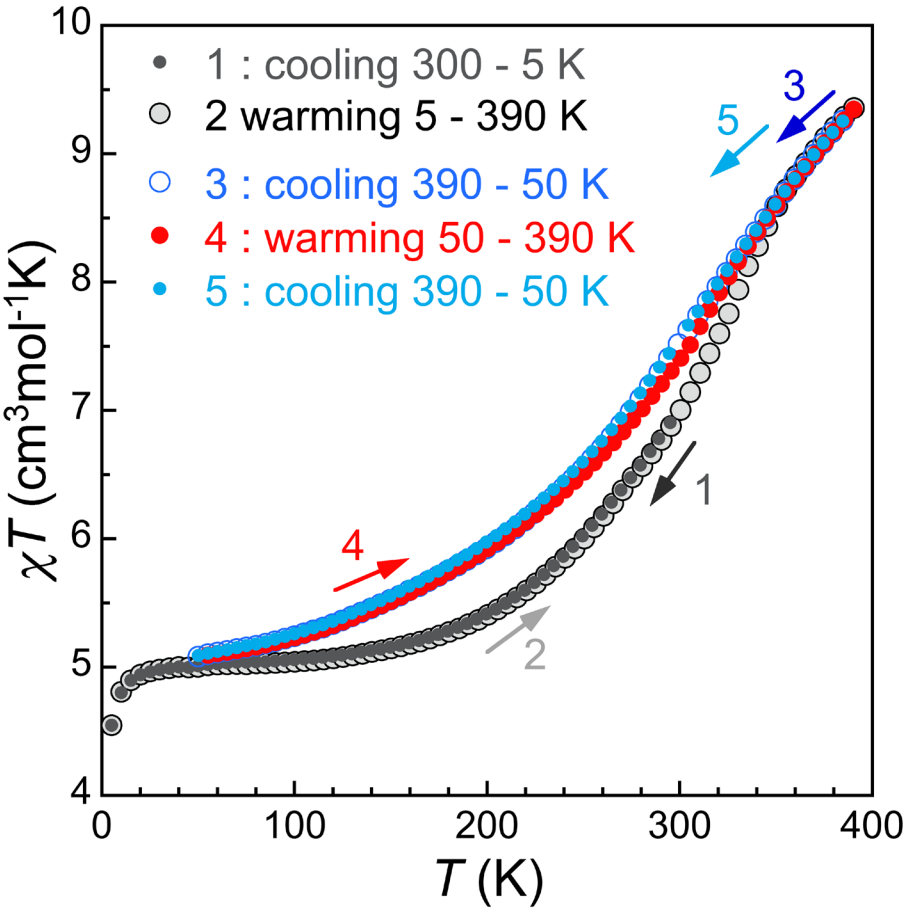

Figure S8. Temperature dependence of χT (χ is the molar magnetic susceptibility) over the indicated cooling-warming-cooling-warming-cooling temperature scan starting at 300 K for a polycrystalline sample of desolvated **1** $[Fe(anilate)_3]@[Fe_2(L2)_3](BF_4)$. The slight difference in the SCO trace after the first warming to 390 K is ascribed to loss of traces of lattice water absorbed from air moist during drying of fresh crystals in air.

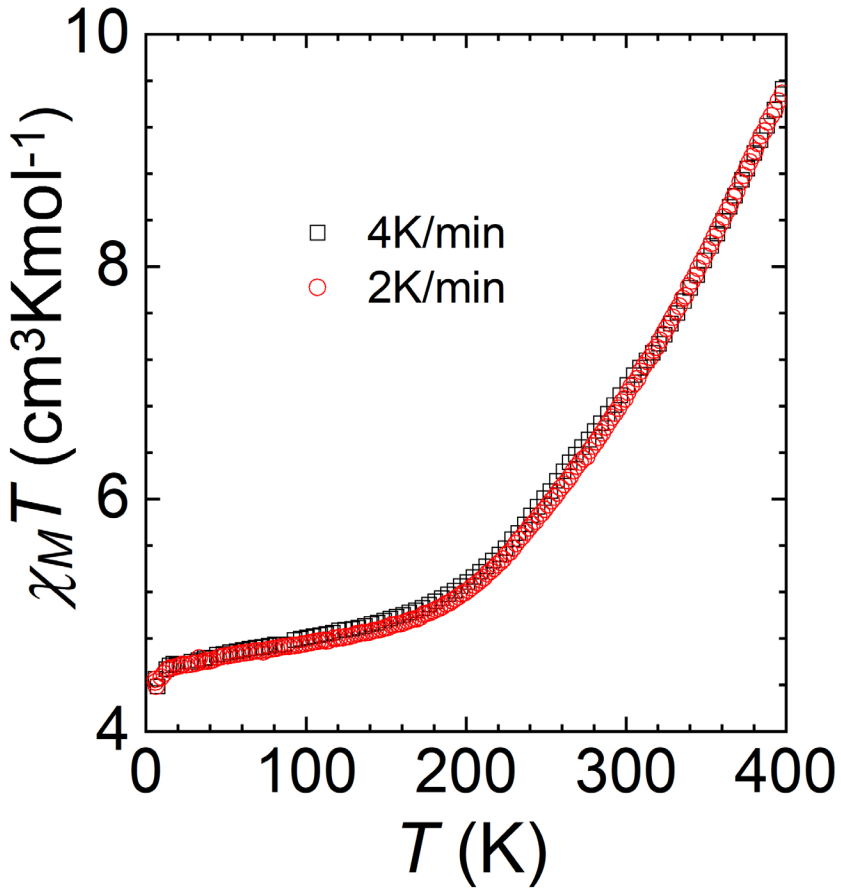

Figure S9. Temperature dependence of χT (χ is the molar magnetic susceptibility) over a 400 to 5 K temperature scan for a polycrystalline sample of desolvated **1** [Fe(anilate)$_3$]@[Fe$_2$(L2)$_3$](BF$_4$) at two different scan rates (as indicated).